Mem. S.A.It. Suppl. Vol. 5, 217

Memorie della
Supplementi

The starburst-AGN connection in ULIRGs

Guido Risaliti[1,2]

[1] INAF - Osservatorio Astrofisico di Arcetri, Largo E. Fermi 5, 50125 Firenze e-mail: risaliti@arcetri.astro.it
[2] Harvard-Smithsonian Center for Astrophysics, 60 Garden Street, Cambridge MA 02138, USA

Abstract. We present the results of L-band spectroscopical observations of local bright ULIRGs, performed with ISAAC at the VLT. The excellent sensitivity of the telescope and of the instrument provided spectra of unprecedented quality for this class of objects, which allowed a detailed study of the relative AGN/starburst contribution to the energy output, and of the composition of the circumnuclear absorber. A new mid-infrared diagnostic diagram is proposed, in which starbursts and AGNs are clearly separated.

Key words. galaxies: active - infrared: galaxies

1. Introduction

Ultraluminous Infrared Galaxies (ULIRGs, $L_{IR} > 10^{12} L_{\odot}$) are the most luminous sources in the local universe, and represent the local counterpart of the class of high-redshift objects dominating the far-infrared and sub-mm background. The huge infrared emission is due to reprocessing by dust of higher frequency radiation, emitted by starburst activity or by an active nucleus.

Several attempts have been made in the last years to understand which of these two sources of energy is dominant in ULIRGs. Known diagnostics involves optical and near-IR spectroscopy (Veilleux, Sanders, & Kim 1999, Veilleux, Kim, & Sanders 1999b, mid-IR imaging and spectroscopy (Genzel et al. 1998), hard X-ray observations (Braito et al. 2003, Ptak et al. 2003), L-band spectroscopy (Imanishi & Dudley 2000). However, none of the above methods can conclusively assess the relative importance of AGN and starburst in a representative sample of objects. This is mainly due to the fact that all the different diagnostic techniques are effective in "extreme" cases, with a clear dominance of one of the two energy sources.

Here we present new L-band spectroscopical results on a sample of bright ULIRGs. We will show that L-band spectra obtained with ISAAC at the VLT can provide a quite effective way to disentangle the AGN from the star formation contributions in ULIRGs. This diagnostics is successful for bright sources, for which independent classification is already present, and can be extended to fainter sources, for which the known diagnostics at other frequencies cannot be used yet, because of insufficient signal-to-noise.

2. L-band diagnostics

L-band low resolution spectra provide a powerful set of diagnostics to investigate the star-

burst/AGN origin of the infrared emission. The main indicators are the following:

- **3.3 μm emission line:** The broad emission feature at 3.3 μm (rest frame) is due to Polycyclic Aromatic Hydrocarbon (PAH) molecules. The excitation of these complex molecules is due to the strong UV continuum produced either by the starburst or the AGN. However, the molecules are easily destroyed by the strong X-ray emission from active nuclei. As a consequence, the observation of a strong 3.3 μm emission feature is an indication that the main source of energy is a starburst. Typical equivalent width for starburst-dominated objects are $EW \sim 100$ nm or more, while in AGN-dominated sources $EW < 20$ nm (Imanishi & Dudley 2000).
- **3.4 μm absorption feature:** The absorption feature at 3.4 μm is due to C-H stretching vibrations in hydrocarbon dust grains (Sandford et al. 1991, Pendleton et al. 1994). In order for this feature to have a significant optical depth ($\tau > 0.2$) a strong point source like an AGN is needed, while the more spread starburst regions would not work (Imanishi & Dudley 2000), unless a huge dust mass or an *ad-hoc* geometry are assumed.
- **Continuum slope:** The continuum slope is expected to be a good indicator of the starburst/AGN contribution. The dust responsible for the IR emission is warmer in AGNs, therefore a steeper spectrum is expected for AGNs. On the other side, the typical starburst spectrum is roughly flat (in a $f_\lambda - \lambda$ plot).

In addition to the physical reasons briefly expained for each of the above indicators, all of them have been confirmed for several bright ULIRGs for which other independent indicators (especially in the hard X-rays, e.g. (Braito et al. 2003)) are available. However, there are important limitations in this diagnostics, which will be discussed in the next Section.

3. Observations and results

The sample chosen for this study is the one of Genzel et al. (1998) consisting of the 15 ULIRGs with IRAS 60 μm flux density $F_{60} >$ 5.4 Jy. Several sources have been already observed in the L-band (3-4 μm) with 4-meter class telescopes in the northern emisphere (Imanishi & Dudley 2000, Imanishi, Dudley, & Maloney 2001). 9 out of 15 objects are visible from the southern emisphere. Our project is to observe these 9 sources with the Infrared Spectrometer and Array Camera (ISAAC) at the VLT. Six spectra have been already obtained. Observations of the remaining 3 are scheduled for July 2004.

Data have been reduced and analyzed using the IRAF package. The results of the spectral analysis is shown in Fig. 1.

The high quality of these spectra allows us to analyze the spectral properties of these sources with unprecedented detail. As an example, in Fig. 2 we plot our highest quality spectrum, relative to the source IRAS 19254-7245. Interestingly, the absorption feature at 3.4 μm can be resolved in substructures due to different hydrocarbon groups. From the relative strength of these single substructures it is possible to estimate the length of the carbon chains, and the frequency of electronegative groups in these molecules. For details, see Risaliti et al. (2003).

The main results of our study are summarized in Table 1, where we also suggest a possible classification based on the indicators discussed above.

It is evident from Table 1 that there are "obvious" cases where all the indicators clearly point to only one of the two energy sources. However, in other cases the situation is less clear. If we consider our sources plus all the other ULIRGs observed in the L-band and with independent starburst/AGN classification, we conclude that the indicators discussed in the previous Section are safe only when they have extreme values: all the sources with very small(< 20 nm) or very large (> 100 nm) EW of the 3.3 μm emission feature are AGN or starburst, respectively; similarly, all the very steep continuum sources, and all the sources with a

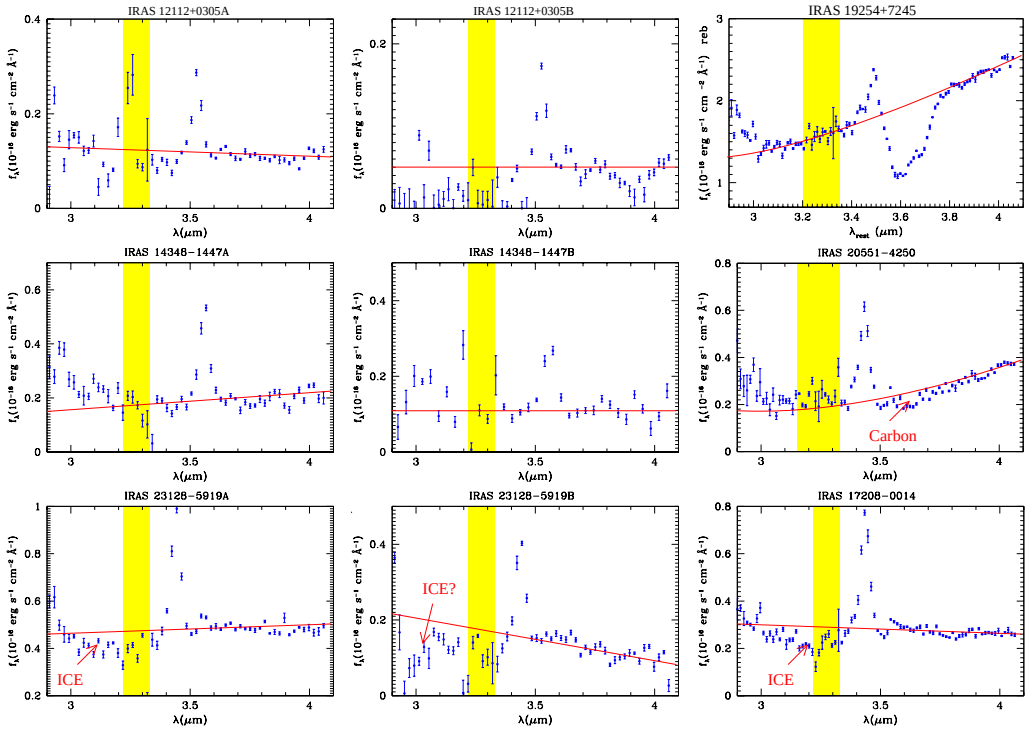

Fig. 1. L-band spectra of our sample of bright ULIRGs. Three sources have resolved double nuclei, for which we plot the spectra separately. The shaded area indicates bad atmospheric transmission. In all spectra the 3.3 μm emission feature is clearly visible (redshifted by $\sim 0.1-0.2$ μm)

Source	Γ^a	EW(3.3μm)^b	τ(3.4 μm)	
IRAS 19254-7245	2.04±0.04	59±6	0.8±0.05	AGN
IRAS 20551-4250	1.84±0.05	113±11	0.2±0.05	AGN
IRAS 14348-1447a	1.49±0.20	185±27	-	SB
IRAS 14348-1447b	0.76±0.59	142±46	-	SB
IRAS 17208-0014	-0.22±0.04	82±4	-	SB
IRAS 23128-5919a	0.56±0.03	69±5	-	AGN
IRAS 23128-5919b	-3.00±0.26	28±8	-	SB
IRAS 12112+0305a	-1.37±0.12	42±2	-	SB
IRAS 12122+0305b	-3.00±0.35	44±6	-	SB

Table 1. Main L-band spectral features of our sample of bright ULIRGs. Three sources have two spatially resolved nuclei. In these cases we report the best fit values for the two components separately. Notes: ^{a}: spectral index in a λ-f$_\lambda$ plot; ^{b}: in units of nm. All errors are at a confidence level of 90%.

deep absorption at 3.4 μm are dominated by AGN emission. In all the other cases, with non-extreme values of any of these indicators, the classification is not clear, as can be seen in Fig. 3 for the continuum slope and the 3.3 μm feature EW.

However, a significant improvement in the diagnostic power of the features discussed

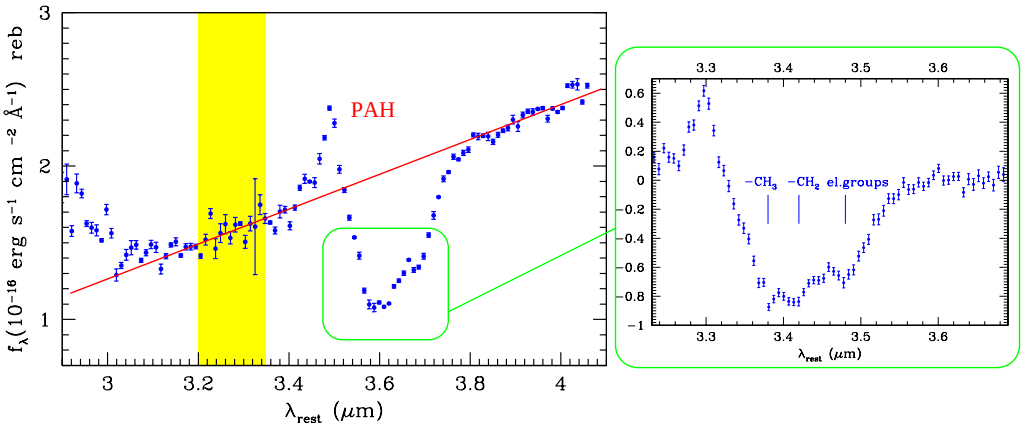

Fig. 2. Details on the ISAAC L-band spectrum of IRAS 19254-7245. The right box shows the substructure of the 3.4 μm absorption feature, which can be used to estimate the length of the carbon chains in the molecules responsible for the absorption (see text and Risaliti et al. 2003).

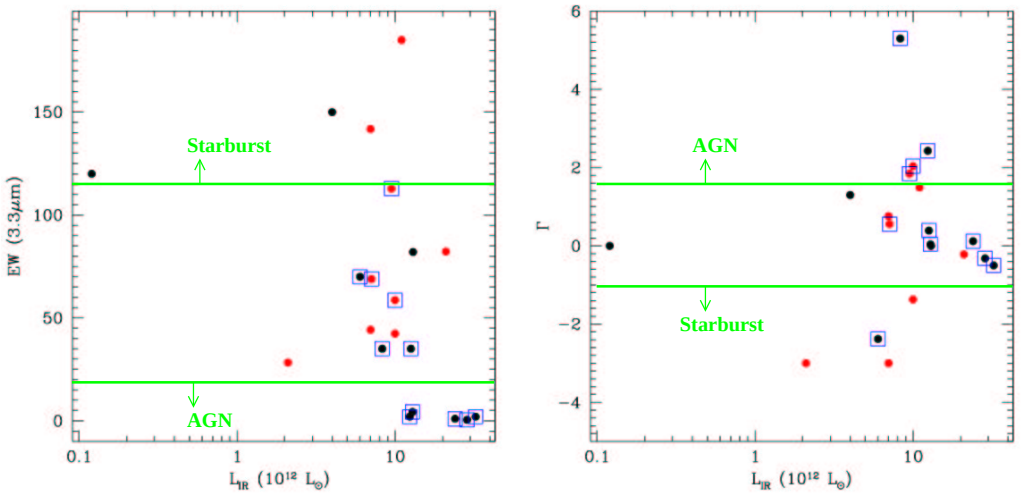

Fig. 3. Left: 3.3 μm emission feature equivalent width versus total infrared luminosity for all the ULIRGs with independent AGN/starburst classification, and L-band spectra. Right: continuum slope (in a $\lambda - f_\lambda$ plot) versus 3.3 μm emission feature equivalent width for the same sources. A starburst/AGN classification based on these single indicators is safe only if their values are extreme.

above can be obtained when two indicators are used at the same time. This is apparent in Fig. 4, where we plot a line in the 3.3 μm EW - continuum slope plane, almost perfectly dividing sources classified as AGNs from those classified as starbursts. The only exception is the heavily absorbed AGN NGC 6240, which appears as starburst dominated at all wavelengths except for the 10-100 keV band, where a powerful AGN dominates the hard X-ray emission (Vignati et al. 1999).

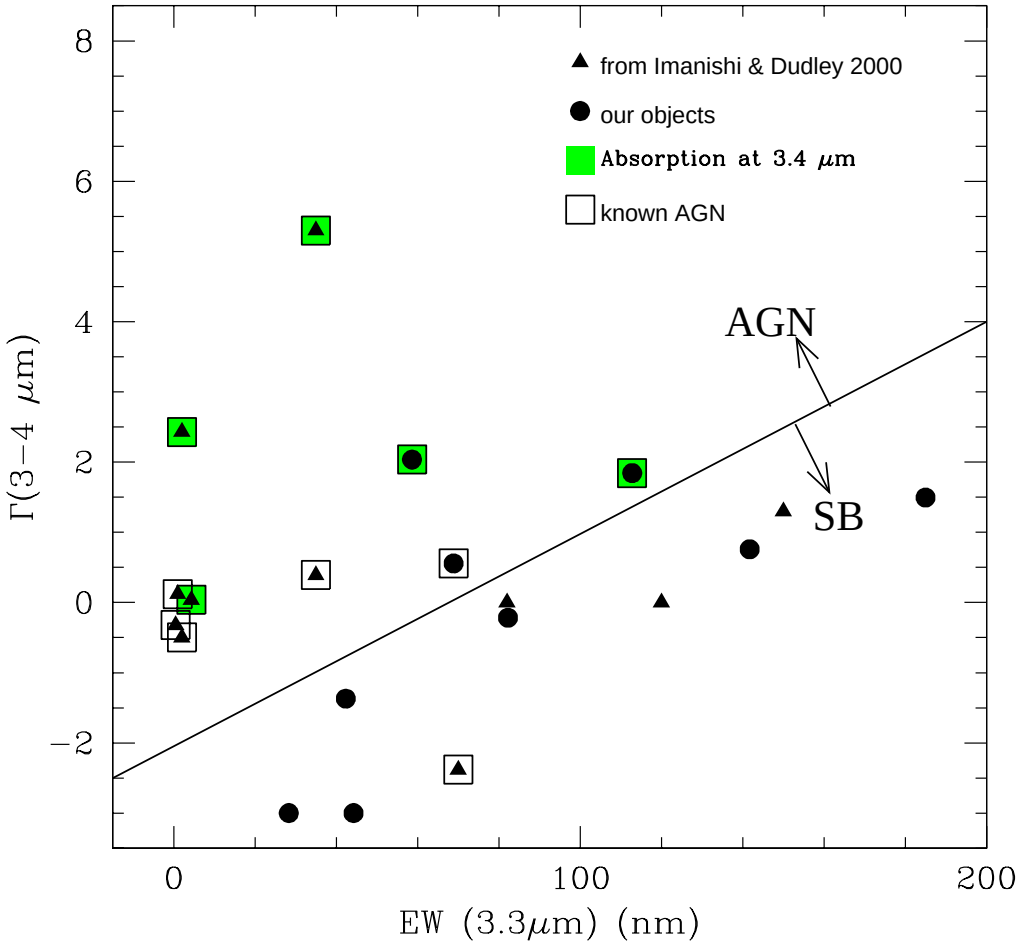

Fig. 4. Continuum slope (in a $\lambda - f_\lambda$ plot) versus 3.3 μm emission feature equivalent width for all the bright ULIRGs with an independent (mostly X-ray) starburst/AGN classification. While the single indicators are not able to distinguish between AGN and starburst in most cases, the combination of the two provides a correct classification in all but one (NGC 6240) cases.

4. Conclusions, and future work

We have presented ISAAC L-band low resolution spectra of a sample of bright ULIRGs. The main results are the following:

– The high sensitivity of ISAAC at VLT allows a study of the main spectral features of bright ULIRGs, with a much higher statistics than in previous works. This means that (a) the brightest object can be studied with unprecedented detail (see, for example, the case of the substructure of the 3.4 μm absorption feature in IRAS 19254-7245); (b) the study of the strongest features can be easily extended to relatively faint objects. Indeed, some of our spectra are among the faintest ever observed (in spectroscopic mode), and many more will

be hopefully observed in the near future (see below).
- The main spectral features detected in our sources are a prominent broad emission line at 3.3 μm, due to reprocessing of UV radiation by PAH molecules, and a power law continuum, with a slope in a large range (between -3 and 2 in a $\lambda - f_\lambda$ plot). An absorption feature at 3.4 μm is detected in two objects.
- We propose a new indicator of the AGN/starburst contribution to the infrared emission of ULIRGs, based on a combination of the continuum slope and the 3.3 μm feature EW. We have shown that all ULIRGs with independent AGN/starburst classification lie in a different region in the plane made by these two parameters (Fig. 3).

The future work based on infrared spectra of ULIRGs will consist in three main steps:

- We will obtain ISAAC L-band spectra for the few still missing ULIRGs in the Genzel et al. (1998) sample.
- For the 3-4 brightest sources, we will extend our study to the 4-5 μm range, in order to study the differences in the continuum emission between starbursts and AGNs.
- Most interesting, we plan to extend our study to as many sources as possible in the 1 Jy ULIRG sample (Kim & Sanders 1998). We will make use of the diagnostics shown in Fig. 3 to obtain a classification for objects which are too faint for any other diagnostics at other wavelengths. In this way it will be possible to have an estimate of the relative AGN/starburst contribution for a sample of ULIRGs much larger than the one available at present ($\sim$ 20 objects).

Acknowledgements. This work is based on observations collected at the European Southern Observatory, Chile (proposal ESO 69.A-0643)

References

Braito, V., et al. 2003, A&A 398, 107
Genzel, R., et al. 1998, ApJ 498, 579
Imanishi, M., & Dudley, C.C. 2000, ApJ 545, 701
Imanishi, M., Dudley, C. C., & Maloney, P. R. 2001, ApJ, 558, L93
Kim, D.-C. & Sanders, D. B. 1998, ApJS 119, 41
Ptak, A., Heckman, T., Levenson, N. A., Weaver, K., & Strickland, D. 2003, ApJ, 592, 782
Risaliti, G., et al. 2003, ApJ, 595, L17
Pendleton, Y. J., Sandford, S. A., Allamandola, L. J., Tielens, A. G. G. M., & Sellgren, K. 1994, ApJ, 437, 683
Sandford, S. A., Allamandola, L. J., Tielens, A. G. G. M., Sellgren, K., Tapia, M., & Pendleton, Y. 1991, ApJ, 371, 607
Veilleux, S., Sanders, D. B., & Kim, D.-C. 1999, ApJ 522, 139
Veilleux, S., Kim, D.-C., & Sanders, D. B. 1999b, ApJ 522, 113
Vignati, P., et al. 1999, A&A 349, L57